ISBN: 978-3-95450-215-8 ISSN: 2226-0366 doi:10.18429/JACoW-LINAC2022-MOPORI22

HIGH-POWER TEST OF AN APF IH-DTL PROTOTYPE FOR THE MUON LINAC

Y. Nakazawa*, H. Iinuma, Ibaraki University, Mito, Ibaraki, Japan
Y. Iwata, National Institute of Radiological Sciences, Chiba, Japan
E. Cicek, H. Ego, K. Futatsukawa, N. Kawamura, T. Mibe, S. Mizobara, M. Otani, N. Saito, T. Yamazaki, M Yoshida, KEK ,Tsukuba, Ibaraki, Japan
Y. Kondo, R. Kitamura, T. Morishita, JAEA, Tokai, Naka, Ibaraki, Japan
Y. Sue, K. Sumi, M. Yotsuzuka, Nagoya University, Nagoya, Japan
Y. Takeuchi, Kyushu University, Fukuoka, Japan
N. Hayashizaki, Tokyo Institute of Technology, Tokyo, Japan
H. Yasuda, University of Tokyo, Hongo, Tokyo, Japan

Abstract

We conducted a high-power test of a prototype cavity of a 324-MHz inter-digital H-mode drift tube linac (IH-DTL) for the muon g-2/EDM experiment at J-PARC. This prototype cavity (short-IH) was developed to verify the fabrication methodology for the full-length IH cavity with a monolithic DT structure. After 40 h of conditioning, the short-IH has been stably operated with an RF power of 88 kW, which corresponds to 10% higher accelerating field than the design field (E_0) of 3.0 MV/m. In addition, the thermal characteristics and frequency response were measured, verifying that the experimental data was consistent with the three-dimensional model. In this paper, the high-power tests of this IH-DTL for muon acceleration are described.

INTRODUCTION

At the Japan Proton Accelerator Research Complex (J-PARC), an experiment is planned to measure the anomalous magnetic moments of muons [1] and search for electric dipole moments using accelerated muons by a muon linear accelerator (linac) [2]. The muon linac consists of a radio-frequency quadrupole linac (RFQ), an inter-digital H-mode drift-tube linac (IH-DTL), disk and washer coupled cavity linacs (DAW-CCL), and disk-loaded accelerating structures (DLS) [3, 4]. Muons are accelerated from an energy of 25 meV to 212 MeV ($\beta = 0.95$), avoiding significant emittance growth to satisfy the experimental requirement of a transverse divergence angle of less than 10^{-5}.

The muons bunched and accelerated by the RFQ are accelerated from 0.34 MeV to 4.3 MeV ($\beta = 0.08 - 0.28$). The Alvarez DTL is widely used for this β region. However, reducing construction costs is critical for the realization of our experiment. Therefore, we employed the alternating phase focusing (APF) [5] method. The APF method utilizes the transverse focusing force derived from the RF electric field by appropriately selecting each gap's positive and negative synchronization phases. With this scheme, the structure can be drastically simplified by omitting the complicated focusing-element-containing drift tubes (DT). The APF is usually used for heavy ion linacs having relatively low beam currents [6–8]. For our muon linac, the beam current is very low, so we considered it applicable. However, more careful treatment of the RF transverse force was necessary in the beam dynamics design [9] because of the much lighter mass of the muon.

Moreover, for the APF IH-DTL cavity, a three-piece structure [10], which is also effective for cost reduction, can be applied. A center plate and two semi-cylindrical side shells made of oxygen-free copper (OFC) are bolted together to form the cavity structure. On the center plate, all DTs are monolithically machined. With this method, the time-consuming DT alignment procedure is not required.

However, because this is the first case that the monolithic DT structure is being applied to a 324 MHz IH-DTL cavity for muon acceleration, we developed a short-length IH-DTL (henceforth called "short-IH") as a prototype. We already confirmed that the field accuracy of less than ±2 %, which is required by the beam dynamics design [11], was achieved only by machining [12]. In this paper, the results of the high power test of short-IH are described.

SHORT-IH

Figure 1 shows the short-IH structure, which corresponds to the upstream one-third of the full-length IH-DTL (full-IH). The short-IH has the same synchronous phase as the first

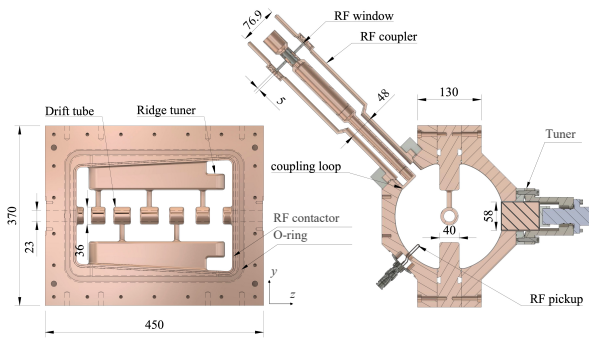

Figure 1: Mechanical structure of the short-IH. (A) Center plate. (B) Cross-sectional view.

* 20nd103s@vc.ibaraki.ac.jp

ISBN: 978-3-95450-215-8 ISSN: 2226-0366 doi:10.18429/JACoW-LINAC2022-MOPORI22

Table 1: Comparison of the full-IH and short-IH

Parameters	Full-IH	Short-IH
Beam pulse width (ns)	10	
Repetition rate (Hz)	25	
RF pulse width (μs)	40	
Resonant frequecy (MHz)	324	
Number of the cells	16	6
Extraction energy (MeV)	4.26	1.30
Cavity length (m)	1.45	0.45
Averaged accelerating field (MV/m)	3.6	3.0
Maximum surface field (MV/m)	35.4	34.7
[E_k : Kilpatrick limit [13]]	2.0 E_k	1.9 E_k
Unloaded Q factor Q_0	10910	8600
Nominal peak power (kW) [100% Q_0]	310	65

six cells of the full-IH, which has 16 cells, and it can accelerate muons from 0.34 MeV to 1.30 MeV ($\beta = 0.08 - 0.15$). Table 1 summarizes the design of the full-IH and short-IH.

The three-piece structure was adopted. Two side shells and a center plate are bolted together, and on the center plate, DTs are monolithically machined, as shown in Fig. 1. Each of them is made of OFC class 1. A coil spring RF contactor made of beryllium copper was installed in the grooves on both sides of the center plate, and the vacuum was sealed with viton O-rings. After the machining, no surface treatments, such as baking, acid rinsing, chemical polishing, or chromate treatment, were applied to reduce the fabrication cost.

The short-IH cavity has three tuner ports, three RF pickup ports, one RF coupler port, and a pumping port with slits [12]. To simplify the tuner structure, no RF contactors were used even under high-power operation. A loop-type RF coupler was used to supply the RF power [14]. The size and default angle of the loop antenna were determined using a low-power coupler [12]. The coupling coefficient of the coupler was set to the critical coupling under high-power operation because the muon beam current is so small that the beam loading is assumed to be negligible.

After the fabrication of the short-IH, low-power tuning were conducted. the frequency was fine-tuned to be 324.00 MHz with the three tuners. The measured unloaded Q factor (Q_0) after the tuning was 7100, which corresponds to 86% of the simulated Q_0. Considering the measured Q_0 , the RF power required for the nominal voltage is 75 kW.

HIGH-POWER TEST

Experimental apparatus The high-power test was conducted at the J-PARC linac building. The RF power from a 324-MHz klystron (Canon E3740A [15]) was applied to the cavity using waveguides (WR2300), coaxial lines (WX203D-77D), and the RF coupler. The cavity was evacuated with a 240-L/s turbo-molecular pump. The vacuum pressure in the cavity was measured using a Bayard-Alpert (BA) gauge, and an interlock was applied to turn off the RF power when the pressure exceeded 1.0×10^{-3} Pa. Three thermocouples were attached to the outer wall of the cavity to measure the cavity temperature, and one thermocouple was placed 2 m away from the cavity to measure the ambient temperature.

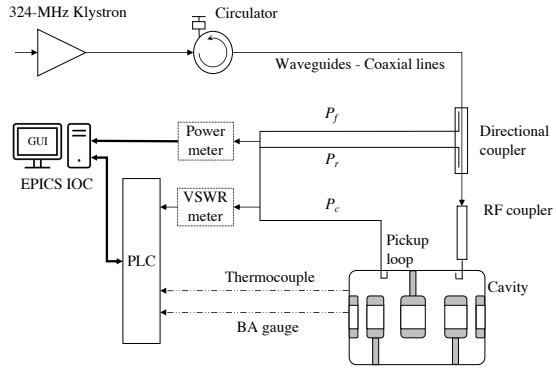

Figure 2: Block diagram of the high-power test system.

Figure 2 shows a block diagram of the high-power test system. A directional coupler was inserted to measure the RF power forward to and reflected from the cavity using power meters [16]. The cavity pickup signal was also measured with the power meter. The data from the power meters were directly recorded by an input/output controller (IOC) of an experimental physics and industrial control system (EPICS). In addition, the RF powers were monitored using the voltage standing wave ratio (VSWR) meters to turn off the RF power in case of excessive reflections.

Conditioning Figure 3 shows the conditioning history. The high-power test was operated only during the daytime, and the horizontal axis of the plot shows the integrated RF-on time. As described in the previous section, no surface

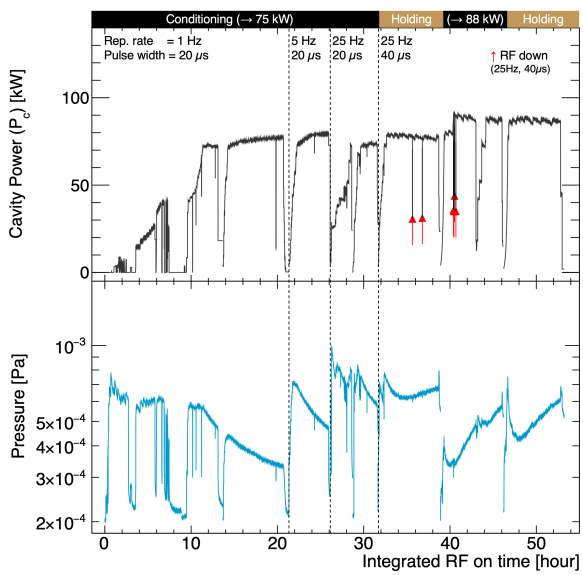

Figure 3: Conditioning history of the cavity power and pressure of the short-IH. Red arrows indicate the cavity trip caused at the nominal duty factor.

ISBN: 978-3-95450-215-8 ISSN: 2226-0366 doi:10.18429/JACoW-LINAC2022-MOPORI22

treatment process was applied, so a lot of gas emissions and discharges occurred at the beginning of the conditioning. Thus, the conditioning was started with a low duty factor (repetition rate of 1 Hz and pulse width of 20 µs), and the power and duty factor were gradually ramped up. As conditioning progressed, the outgases steadily decreased. It took 32 h from the start of the conditioning to achieve a nominal duty factor of 0.1% (25 Hz, 40 µs) and the required peak power of 75 kW, considering the measured Q_0.

After reaching the optimum nominal power and duty factor, holding tests with nominal and increased accelerating field were conducted. The cavity trip occurred only twice during the 7-h holding test with nominal power. During the 7-h operation with 88 kW, which corresponds to 10% increased voltage, there was no trip. From these results, even though no surface treatment was applied and RF contactor-less movable tuners were used, it is confirmed that the short-IH can be operated quite stably after following the appropriate conditioning process.

Thermal characteristics The thermal characteristics of the short-IH were measured and compared to the results of a three-dimensional finite element method (FEM) analysis. The temperature distribution and deformation due to the power dissipation were analyzed using `CST MICROWAVE STUDIO` and `MPHYSICS STUDIO` [17]. To simplify the calculation, detailed structures of components such as slug tuners and RF contactors are omitted in this analysis.

First, the transient temperature distribution in the cavity was derived using the simulated power dissipation, as shown in Fig. 4 (a). Here, the heat transfer coefficient at the surface of the cavity outer wall is set to $8\,\mathrm{W/m^2 \cdot K}$ assuming natural convection to the atmosphere [18]. Then, using the temperature distribution, the deformation and frequency shift response were calculated.

Figure 4 (b) shows the measured and simulated transient behavior of frequency shift (Δf) from 324 MHz for an RF power of 88 kW. The horizontal axis represents the time after RF power is turned on. The measured and simulated data were fitted with $\Delta f \propto (e^{\tau_1^{-1}} + e^{\tau_2^{-1}})$. The measured frequency were consistent with the simulation results within several tens of kHz. Moreover, the two measured time constants were also consistent with the simulation results. Figure 4 (c) represents the temperature drift of the cavity. The temperatures of the three thermocouples attached to the outer wall of the cavity were averaged, and their differences from the ambient temperature were plotted. The measured temperature of the outer cavity wall was in good agreement with the simulation result. In the simulation, the temperatures of the DTs increase with quicker time constants than the temperature of the outer wall during t = 0 ~ 0.3 h because the heat capacities of the DTs are smaller than that of the cavity wall. This result indicates that the two time constant are derived from the DT's local deformation and the entire cavity's thermal expansion, respectively. These results prove the validity of the simulations of the IH-DTL.

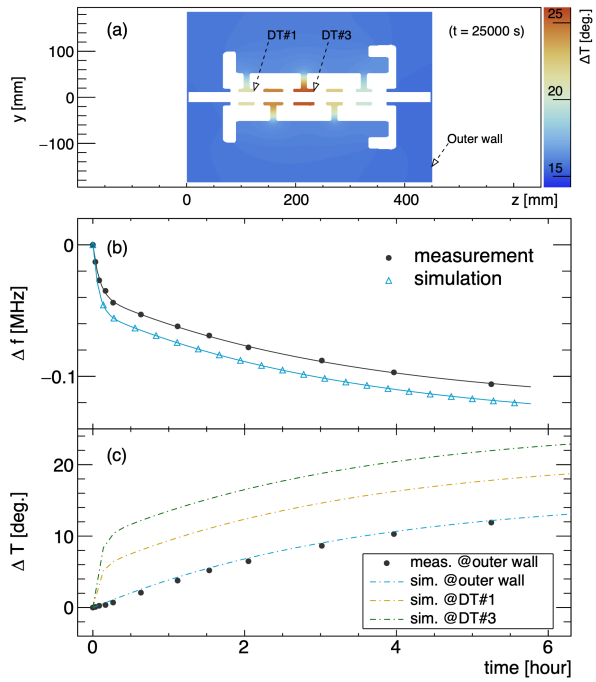

Figure 4: (a) Simulated temperature distribution with the RF power of 88 kW. (b) Frequency shift as functions of time after the RF power of 88 kW was turned on. Solid lines show the fitting results. (c) Temperature drift as functions of time. The data indicates the difference between ambient and cavity surface temperatures. The dotted lines show the simulated temperatures of the first and third DTs and outer wall.

SUMMARY

A high-power test of an APF IH-DTL (short-IH) for the muon linac was successfully conducted. After 40 h of conditioning, the peak power reached 88 kW, corresponding to a 10% higher accelerating field than the design field. We demonstrated that even though no surface treatment was applied, the short-IH could be operated very stably. Moreover, the transient behavior of temperatures and frequency were measured and compared with the 3D FEM model. The measured frequency shift was consistent with simulations to within several percent. This study proves that the design and fabrication methodology established by the short-IH can be applied to the full-IH required for the realization of the new muon g-2/EDM experiment.

ACKNOWLEDGEMENTS

This work was supported by JSPS KAKENHI grant numbers JP15H03666, JP18H03707, JP16H03987, JP16J07784, JP20J21440, JP20H05625, JP21K18630, JP21H05088, JP22H00141; the JST FOREST Program (grant number JPMJFR212O); and the natural science grant of the Mitsubishi Foundation. This paper is based on results obtained from a project commissioned by the New Energy and Industrial Technology Development Organization (NEDO).

ISBN: 978-3-95450-215-8 ISSN: 2226-0366 doi:10.18429/JACoW-LINAC2022-MOPORI22

REFERENCES

[1] T. Aoyama *et al.*, "The anomalous magnetic moment of the muon in the Standard Model" Physics Reports 887, p. 1, 2020.

[2] M. Abe *et al.*, "A new approach for measuring the muon anomalous magnetic moment and electric dipole moment", Prog. Theor. Exp. Phys., p. 053C02, 2019. doi:10.1093/ptep/ptz030

[3] Y. Kondo *et al.*, "Re-Acceleration of Ultra Cold Muon in JPARC Muon Facility", presented at IPAC'18, Vancouver, Canada, April-May, 2018, , pp. 5041–5046. doi:10.18429/JACoW-IPAC2018-FRXGBF1

[4] M. Otani *et al.*, "First muon acceleration and muon linear accelerator for measuring the muon anomalous magnetic moment and electric dipole moment", *Progress of Theoretical and Experimental Physics*, vol. 2022, p. 052C01, 2022. doi:10.1093/ptep/ptac067

[5] S. Minaev and U. Ratzinger, "APF or KONUS drift tube structures for medical synchrotron injectors - A comparison", in *Proc. 18th Particle Accelerator Conference*, New York, pp. 3555–3557, 1999).

[6] Y. Iwata *et al.*, "Alternating-phase-focused IH-DTL for an injector of heavy-ion medical accelerators", *Nucl. Intrum. Methods Phys. Res., Sect. A*, vol. 569, pp.685–696, 2006. doi:10.1016/j.nima.2006.09.057

[7] Y. Iwata *et al.*, "Performance of a compact injector for heavy-ion medical accelerators", *Nucl. Intrum. Methods Phys. Res., Sect. A*, vol. 572, pp.1007–1021, 2007. doi:10.1016/j.nima.2006.09.057

[8] P. F. Ma *et al.*, "Development of a compact 325 MHz proton interdigital H-mode drift tube linac with high shunt impedance", *Phys. Rev. Accel. Beams*, vol. 24, p. 020101, 2021. doi:10.1103/PhysRevAccelBeams.24.020101

[9] M. Otani *et al.*, "Interdigital H-mode drift-tube linac design with alternative phase focusing for muon linac", *Phys. Rev. Accel. Beams*, vol. 19, p. 040101, 2016. doi:10.1103/PhysRevAccelBeams.19.040101

[10] Time incorporated company, Japanese Patent No. 5692905 (P5692905) (2015).

[11] M. Otani *et al.*, "Inter-digital H-mode drift-tube linac design with alternative phase focusing for muon linac", in *Proceedings of the 13th Meeting of Particle Accelerator Society of Japan (PASJ'16)*, p. 858, 2016.

[12] Y. Nakazawa *et al.*, "Development of Inter-Digital H-Mode Drift-Tube Linac Prototype With Alternative Phase Focusing for a Muon Linac in the J-PARC Muon G-2/EDM Experiment", *Journal of Physics: Conference Series*, vol. 1350, p. 012054, 2019. doi:10.1088/1742-6596/1350/1/012054

[13] W. D. Kilpatrick, "Criterion for Vacuum Sparking Designed to Include Both rf and dc", *Review of Scientific Instruments*, vol. 28, p. 824, 1957. doi:10.1063/1.1715731

[14] Y. Nakazawa *et al.*, "Multipacting Simulations of Coaxial Coupler for IH-DTL Prototype in Muon Accelerator", in *Proc. 3rd J-PARC Symposium*, p.011128, 2019. doi:10.7566/JPSCP.33.011128

[15] Canon electron tubes and devices, Canon E3740A.

[16] Spanawave, Model 8542C Dual Input Universal Power Meter. http://www.spanawave.com/store/index.asp

[17] Computer Simulation Technology, CST Studio Suite. https://www.cst.com/products/CSTMWS

[18] P. Kosky *et al.*, Chapter 14- mechanical engineering, in Exploring Engineering (Fifth Edition), pp317-340 (2021).